THE JOURNAL OF BIOLOGICAL CHEMISTRY VOL. 287, NO. 27, pp. 23119–23127, June 29, 2012

A Highly Conserved Cytoplasmic Cysteine Residue in the α4 Nicotinic Acetylcholine Receptor Is Palmitoylated and Regulates Protein Expression*[S]

Received for publication, November 28, 2011, and in revised form, May 7, 2012 Published, JBC Papers in Press, May 16, 2012, DOI 10.1074/jbc.M111.328294

Stephanie A. Amici[‡1], Susan B. McKay[‡], Gregg B. Wells[§], Jordan I. Robson[‡], Muhammad Nasir[‡], Gerald Ponath[‡], and Rene Anand[‡¶2]

From the Departments of [‡]Pharmacology and [¶]Neuroscience, College of Medicine, The Ohio State University, Columbus, Ohio 43210 and the [§]Department of Molecular and Cellular Medicine, College of Medicine, Texas A&M Health Science Center, College Station, Texas 77843

Background: The mechanisms underlying nicotinic acetylcholine receptor (nAChR) trafficking are unclear.
Results: Cysteine mutations within cytoplasmic loops of the α4 nAChR subunit change surface and total receptor expression, and a cysteine in the first loop is palmitoylated.
Conclusion: α4 nAChR intracellular cysteines influence receptor stability and trafficking.
Significance: Identifying the determinants of nAChR trafficking will provide insight into nAChR biology.

Nicotinic acetylcholine receptor (nAChR) cell surface expression levels are modulated during nicotine dependence and multiple disorders of the nervous system, but the mechanisms underlying nAChR trafficking remain unclear. To determine the role of cysteine residues, including their palmitoylation, on neuronal α4 nAChR subunit maturation and cell surface trafficking, the cysteines in the two intracellular regions of the receptor were replaced with serines using site-directed mutagenesis. Palmitoylation is a post-translational modification that regulates membrane receptor trafficking and function. Metabolic labeling with [^{3}H]palmitate determined that the cysteine in the cytoplasmic loop between transmembrane domains 1 and 2 (M1–M2) is palmitoylated. When this cysteine is mutated to a serine, producing a depalmitoylated α4 nAChR, total protein expression decreases, but surface expression increases compared with wild-type α4 levels, as determined by Western blotting and enzyme-linked immunoassays, respectively. The cysteines in the M3-M4 cytoplasmic loop do not appear to be palmitoylated, but replacing all of the cysteines in the loop with serines increases total and cell surface expression. When all of the intracellular cysteines in both loops are mutated to serines, there is no change in total expression, but there is an increase in surface expression. Calcium accumulation assays and high affinity binding for [^{3}H]epibatidine determined that all mutants retain functional activity. Thus, our results identify a novel palmitoylation site on cysteine 273 in the M1-M2 loop of the α4 nAChR and determine that cysteines in both intracellular loops are regulatory factors in total and cell surface protein expression of the α4β2 nAChR.

Neuronal nicotinic acetylcholine receptors (nAChRs)[3] are part of the Cys-loop family of ligand-gated cationic channels. They are assembled from different combinations of α2–α10 and β2–β4 subunits to form pentameric receptors (1). The subunit structure contains four transmembrane domains giving rise to two cytoplasmic loops, a small linker region between the first and second transmembrane domains (M1-M2) and a large loop between the third and fourth transmembrane domains (M3-M4) varying in size between the subunits, with the α4 nAChR subunit containing the largest loop. The M3-M4 intracellular loop of the rat α4 nAChR subunit contains specific leucine residues that are critical for trafficking the receptor to the cell surface (2) and also contains a motif necessary for receptor targeting to axons (3). However, the mechanisms underlying trafficking and targeting remain unclear.

Protein *S*-palmitoylation is a reversible, covalent attachment of the 16-carbon fatty acid, palmitate, to cysteine residues on proteins by thioester bond formation. It is a dynamic post-translational modification that plays a role in the trafficking of many soluble and membrane proteins, including nAChRs, through the secretory pathway to the cell surface, localization in specific membrane domains at the surface, and internalization, recycling, and/or degradation (for review, see Refs. 4–7). In neurons, palmitoylation modulates growth cone formation and neurite outgrowth (8), presynaptic vesicle fusion (9), and postsynaptic signal transduction (10).

The muscle-type nAChR was the first receptor type found to be palmitoylated on both the α and β nAChR subunits (11). More recently, the neuronal α7 and α4β2 nAChRs have been shown to be palmitoylated (12, 13), but the specific palmitoyla-

* This work was supported in part by National Institutes of Health Grant RO1 DA019675 (to R. A.) from the National Institute on Drug Abuse and the Ohio State University College of Medicine Medical Research Fund.
[S] This article contains supplemental "Experimental Procedures."
[1] Recipient of Ruth Kirschstein National Research Service Award F32 DA026240 from the National Institute on Drug Abuse.
[2] To whom correspondence should be addressed: Dept. of Pharmacology, College of Medicine, The Ohio State University, 460 W. 12th Ave., Rm. 796, Columbus, OH 43210. Tel.: 614-292-1380; Fax: 614-292-7544; E-mail: Rene.Anand@osumc.edu.

[3] The abbreviations used are: nAChR, nicotinic acetylcholine receptor; DIV, days *in vitro*; IP, immunoprecipitation; 2-BP, 2-bromopalmitate; DMSO, dimethyl sulfoxide; ANOVA, analysis of variance.

tion sites have not been identified. We exchanged all of the cysteines with serines in the intracellular loops of the α4 nAChR subunit to determine the role of cysteine modifications, including palmitoylation, on the expression and trafficking of the α4 nAChR subunit. Within the M1-M2 region, there is a single cysteine residue, whereas the M3-M4 loop contains 11 cysteine residues. The cysteine in the M1-M2 loop is palmitoylated and is conserved in the α2, α3, α4, α6, β2, and β4 nAChR subunits. The homologous cysteine previously has been associated with use-dependent inactivation of α3-containing nAChRs in hyperglycemic and oxidative conditions (14). When this cysteine is mutated to a serine, creating a depalmitoylated mutant, total protein expression is decreased, whereas cell surface expression increases. The cysteine to serine mutations in the M3-M4 cytoplasmic loop lead to increased total and cell surface protein expression. When all of the cysteines are mutated to serines in both cytoplasmic domains, there is no change in total protein expression, but surface expression is increased. Functional activation, ligand-binding affinity, and targeting to presynaptic terminals of the mutant α4β2 nAChRs do not vary from wild-type (WT) α4 nAChR subunits. Our results suggest that cysteine residues modulate both total and surface protein expression of the α4 nAChR subunit.

EXPERIMENTAL PROCEDURES

Constructs—All constructs were made by PCR using appropriate pairs of forward and reverse synthetic oligonucleotide primers (Invitrogen) and *PfuTurbo* DNA polymerase (Agilent Technologies, Santa Clara, CA). The rat α4 nAChR subunit containing an N-terminal FLAG tag and the untagged β2 nAChR subunit cDNAs were cloned into the mammalian cell expression vector, C-terminal p3xFLAG-CMV vector (Sigma). Mutagenesis of the α4 nAChR subunit was performed using the QuikChange site-directed mutagenesis kit (Agilent Technologies). Three mutant constructs were generated in the α4 nAChR: 1) a cysteine to serine mutation within the M1-M2 loop (α4C273S), 2) 11 mutations within the M3-M4 loop (α4ΔC), and 3) mutation of all cysteines within the M1-M2 and M3-M4 loops (α4ΔΔC). For the α4ΔΔC mutant, the α4ΔC plasmid backbone was used with the α4C273S primers to generate a mutant lacking all of the intracellular cysteines (see supplemental "Experimental Procedures" for primer pairs).

Antibodies—The following antibodies were used: rat monoclonal antibody (mAb) to the β2 nAChR subunit (mAb 295) (kindly provided by Dr. J. Lindstrom, University of Pennsylvania, Philadelphia, PA); mouse mAb against FLAG tag (1:1000, F-3165, Sigma); a goat polyclonal Ab against the β2 nAChR subunit (1:100, C-20, sc-1449, Santa Cruz Biotechnology, Santa Cruz, CA) that binds to denatured β2 subunits on immunoblots; rabbit polyclonal anti-GAPDH Ab (1:5000, G-9545, Sigma), rabbit polyclonal Ab against vesicular stomatitis virus-G (1:2000, Sigma), and a mouse monoclonal Ab against HA (1:2000, Abcam, Cambridge, MA). Goat anti-rat, anti-mouse, and anti-rabbit horseradish peroxidase-conjugated secondary Abs were obtained from Pierce. The Alexa Fluor 488-, Alexa Fluor 594-, and Alexa Fluor 647-conjugated goat anti-rat, goat anti-rabbit, and goat anti-mouse secondary Abs were obtained from Molecular Probes (Invitrogen).

tsA 201 Cell Culture—Human tsA 201 cells, a derivative of the HEK cell line 293, were cultured in DMEM (Invitrogen) supplemented with 10% FBS (HyClone, Thermo Scientific, Logan, UT) and 20 μg/ml gentamicin (Invitrogen) as described previously (2). tsA 201 cells were transfected using Lipofectamine 2000 according to the manufacturer's instructions (Invitrogen). For all experiments, tsA 201 cells were plated on day 1 and transfected on day 2, medium was exchanged on day 3, moved to 30 °C to promote assembly of α4β2 nAChRs on day 4, and used for experiments on day 5.

Primary Hippocampal Neuron Culture—Cultures were prepared and maintained as described previously (15). Neurons were transfected at 7–10 days *in vitro* (DIV) using the Clontech CalPhos Mammalian Transfection Kit (BD Biosciences) as described (16).

Neuron/tsA 201 Cell Coculture Experiments—Experiments were performed as described previously (15). After 24 h, transfected tsA 201 cells were coplated at 15,000 cells/well with the neurons, transferred to 30 °C (12–13 DIV), and processed for immunocytochemistry at 14–15 DIV.

Metabolic Labeling of nAChRs with [^{3}H]Palmitate—tsA 201 cells were transfected with α4, α4ΔC, α4ΔΔC, or α4C273S. On the day of the experiment, medium was exchanged for starvation (DMEM containing 1% fatty acid-free BSA), incubated at 37 °C for 30 min, and then metabolically labeled in starvation medium containing 1 millicurie/ml [^{3}H]palmitate (PerkinElmer Life Science) for 4 h at 37 °C. The cells were washed in PBS and lysed in solubilization buffer (50 mM NaCl, 5 mM Tris, pH 8.0, 5 mM EDTA, 5 mM EGTA, 2% Triton X-100) with aprotinin, leupeptin, and pepstatin (all at 5 μg/ml), 1 mM PMSF, 1 mM benzamidine, and 1× phosphatase inhibitor cocktails 1 and 2 (Sigma), and solubilized for 2 h at 4 °C. The lysates were spun for 15 min at 16,000 × *g*, and the supernatants were transferred to new tubes. The α4 FLAG-tagged subunits were captured by immunoprecipitation (IP) using the FLAG M2 beads (Sigma) as described previously (2). For the hydroxylamine experiment, FLAG M2 beads were treated with 1 M hydroxylamine (Sigma) or control 1 M Tris-HCl, pH 7.4 for 1 h. 10% of the IP eluates (5 μl) were run on a 7.5% SDS-PAGE, transferred to PVDF, and blotted with anti-FLAG or anti-C-20 antibodies. The remaining 90% of IP eluates were run on a parallel blot that was stained with Coomassie Brilliant Blue (Bio-Rad Laboratories), destained (50% methanol, 10% acetic acid), incubated with Amplify (GE Healthcare) for 30 min, dried under vacuum at 80 °C for 2 h, exposed to film (Kodak BioMax MS) at −80°C for 21 days and then developed.

Pulldowns from Transfected tsA 201 Cells—Transfected tsA 201 cells were solubilized in 2% Triton X-100 buffer for 2 h at 4 °C and captured by IP using FLAG M2 beads as described previously (2).

Immunoblotting—Following separation using SDS-PAGE, proteins were transferred onto PVDF membrane and incubated with diluted Abs in PBS containing 3% nonfat milk powder. The binding of the primary Abs to proteins was detected using appropriate secondary Abs as described previously (2). Blots were scanned and analyzed in ImageJ software. α4 nAChR subunit expression was normalized to GAPDH ($n = 5$).

Immunostaining and Imaging—Transfected tsA 201 cells were washed and fixed in Hanks' balanced salt solution (with Ca^{2+} and Mg^{2+}) supplemented with 4% paraformaldehyde and 4% sucrose, pH 7.4 (15 min, room temperature), blocked with Hanks' balanced salt solution containing 3% normal goat serum and 3% BSA (for surface immunocytochemistry) or blocked with Hanks' balanced salt solution containing 3% normal goat serum, 3% BSA, and 0.2% Triton X-100 (for total immunocytochemistry) (30 min at room temperature), and incubated with the appropriate primary (2 h, 4 °C) and secondary (90 min at room temperature) antibodies. Coverslips were mounted onto slides with ProLong Gold Antifade Reagent (Invitrogen).

For the mixed neuron/tsA 201 cell assays, the cultures were processed as described previously (15). They were fixed, blocked, and incubated with the appropriate primary (2 h, 4 °C) and secondary (90 min, room temperature) antibodies.

Cells and cocultures were visualized as described (15). Single-plane fluorescence images were captured using a Hamamatsu EM camera, and images were processed using the Slide Book software (version 4.2). Figures were processed with Adobe Photoshop CS5 Extended (Adobe Systems, Inc., San Jose, CA).

Enzyme-linked Immunoassay for Quantitating Cell Surface α4β2 nAChRs—Transfected tsA 201 cells were plated in 12-well dishes and analyzed for cell surface expression of α4β2 nAChRs using the methodology described previously (2). Surface expression was detected with a rat mAb against the β2 nAChR subunit (mAb 295) whose epitope is located in the extracellular domains of the subunit. The nonspecific background binding of antibodies to cells was determined by expressing the β2 nAChR subunit alone. To inhibit palmitoylation, medium was replaced with fresh medium containing either 2-bromopalmitate (2-BP, 120 μM, Sigma) or an equivalent volume of DMSO as a vehicle control on day 4.

Fluorescence Calcium Accumulation Assays—tsA 201 cells were transiently transfected with plasmid DNA for the β2 nAChR subunit and either WT α4, α4ΔC, α4ΔΔC, or α4C273S subunits. After 48 h at 37 °C, the cells were plated onto 96-well plates at a density of 1×10^5 cells per well, and moved to 30 °C overnight. The cells were washed twice with HEPES buffered Krebs-Saline solution (155 mM NaCl, 4.6 mM KCl, 1.2 mM $MgSO_4$, 1.8 mM $CaCl_2$, 6 mM glucose, 20 mM HEPES, pH 7.2), loaded with calcium 5 NW dye (Molecular Devices, Sunnydale, CA), and incubated for 1 h at room temperature in the dark. Fluorescence was measured at 0.7-s intervals for 2 min per well using a fluorescence plate reader (FLEXstation, Molecular Devices) at an excitation of 494 nm and an emission of 525 nm. Fluorescence was recorded for 60 s before stimulation and 60 s after stimulation with various concentrations of epibatidine. Functional responses were quantified by first calculating the net fluorescence change (the difference between control, nonstimulated groups, and agonist-treated groups). Results were expressed as a percentage of maximal agonist group responses. Curve fitting was generated using Prism software (GraphPad Software, Inc., San Diego, CA).

Ligand Binding Studies—[^{3}H]Epibatidine binding to α4β2 nAChRs was done directly in wells as described previously (2). For inhibition experiments, cells were incubated with 400 pM [^{3}H]epibatidine in the presence or absence of 10, 30, 100, 300, or 1000 nM nicotine overnight at 4 °C. The bound epibatidine was eluted in 0.5% SDS, 0.5 M NaOH for 1 h. The eluates were mixed with liquid scintillation fluid, and the amount of radioactivity present was measured in a LS6500 (Beckman Coulter, Brea, CA). Background binding was determined using untransfected cells and was subtracted from the amount of radioactivity in eluates. The data shown were normalized to the amount bound in the absence of nicotine.

Calculations and Statistics—For cell surface binding assays and total protein analyses, the difference between groups was analyzed statistically by paired *t* test in Excel. For calcium accumulation and ligand binding assays, curves were fitted using Prism 5 software. Half-maximal effective (EC_{50}) values were derived from the sigmoidal dose-response equation, $Y = 100/(1 + 10((\log EC_{50} - X)\cdot HS))$, and half-maximal inhibitory (IC_{50}) values were derived from the sigmoidal dose-response equation, $Y = 100/(1 + 10((\log IC_{50} - X)\cdot HS))$, where Y is the percentage of the maximal effect at a given concentration (X), and HS is the Hill slope (HS = 1 was used for these calculations). The K_i values were determined using the one site − fit K_i equation in Prism 5, $Y = \text{bottom} + (\text{top} - \text{bottom})/(1 + 10\wedge(X - \log EC_{50}))$, where $\log EC_{50} = \log(10\wedge \log K_i \cdot (1 + \text{radioligandNM}/\text{Hot}K_d\text{NM})$ and radioligandNM = 0.40 nM and HotKdNM = 0.015 nM (17). The EC_{50} and K_i values were compared between the groups by one-way ANOVA. All results were expressed as means ± S.E.

RESULTS

α4 nAChR Is Palmitoylated at Cysteine 273 in M1-M2 Intracellular Loop—To determine the functional roles of cysteines within the α4 nAChR subunit, we used site-directed mutagenesis to replace the cysteine residues with serine residues in the α4 nAChR cytoplasmic loops. We made three mutant constructs: α4C273S, in which the single cysteine in the M1-M2 loop was replaced with a serine; α4ΔC, in which all 11 cysteines in the M3-M4 loop were replaced with serines; and α4ΔΔC, in which all 12 cysteines in both loops were replaced with serines (Fig. 1*A*).

Our initial hypothesis was that the M3-M4 loop contained one or more palmitoylation sites, so tsA 201 cells were transiently transfected with N-terminally FLAG-tagged WT α4 or the α4ΔC cysteine mutant nAChR subunits in the absence or presence of the untagged β2 nAChR subunit and metabolically labeled with [^{3}H]palmitate, captured by IP with FLAG M2 beads, separated by SDS-PAGE, dried, and exposed to film (Fig. 1*B*). Both the α4 and β2 nAChR subunits were labeled metabolically with [^{3}H]palmitate (Fig. 1*B*, *top* autoradiograph, *lanes 1* and *2*), as observed previously (13). The α4 nAChR subunits are labeled in the absence or presence of the β2 nAChR subunits (Fig. 1*B*). Surprisingly, cells transfected with the α4ΔC did not incorporate a detectably reduced amount of [^{3}H]palmitate compared with the α4 nAChR subunit, suggesting that none of the cysteines in the M3-M4 loop were palmitoylated (Fig. 1*B*, *lanes 3* and *4*). One-tenth of the IP eluate was run on a parallel SDS-PAGE and immunoblotted for IP capture efficiency with anti-FLAG antibody to detect the α4 nAChR subunit and with

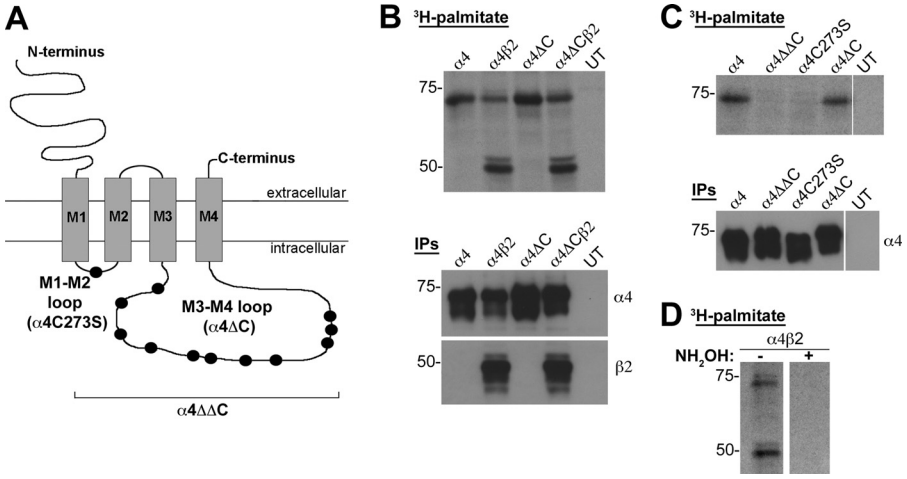

FIGURE 1. **The α4 nAChR subunit is palmitoylated at Cys^{273}.** *A*, schematic of the α4 nAChR subunit, identifying the cysteines in the cytoplasmic loops that were mutated to serine residues: M1-M2 loop (C273S); and M3-M4 loop (C370S, C401S, C412S, C425S, C446S, C452S, C488S, C496S, C533S, C535S, C537S). *B–D*, tsA 201 cells were transiently transfected with N-terminally FLAG-tagged α4 (*lane 1*), α4 and β2 (*lane 2*), α4ΔC (*lane 3*), or α4ΔC and β2 (*lane 4*) nAChR subunits (*B* and *D*) or with N-terminally FLAG-tagged α4, α4ΔΔC, α4C273S, or α4ΔC nAChR subunits (*C*). *UT* denotes untransfected cells processed in parallel as a control (*B* and *C*). The cells were metabolically labeled with 1 millicurie/ml [^{3}H] palmitate, solubilized, and the FLAG-tagged subunits were captured by IP with FLAG M2 beads. The IP eluates were separated by SDS-PAGE, dried under vacuum, exposed to film at −80 °C, and developed after 21 days (*B* and *C*, *top panels*). 5 μl of IP eluate (10% of total IP) was run on a SDS-PAGE and analyzed by Western analysis using anti-FLAG antibody and anti-β2 antibody (*B* and *C*, *bottom panels*). *D*, lysates from α4β2 expressing cells were treated with 1 M Tris-HCl (control) or 1 M hydroxylamine (NH_2OH) to confirm thioester linkage to intracellular cysteines. Molecular mass is in kDa along the *left side* of the blot.

anti-C20 antibody to detect the β2 nAChR subunit (Fig. 1*B*, *bottom* blots).

Because [^{3}H]palmitate incorporation was similar between the WT α4 and the α4ΔC mutant nAChR subunit, the α4, α4ΔC, α4ΔΔC, and α4C273S nAChR subunits were transfected and metabolically labeled with [^{3}H]palmitate. The α4 and α4ΔC nAChR subunits were labeled (Fig. 1*C*, *lanes 1* and *4*), but the α4ΔΔC and the α4C273S mutant did not incorporate [^{3}H]palmitate (Fig. 1*C*, *lanes 2* and *3*), indicating that Cys^{273} is the only cysteine in the α4 nAChR subunit that is palmitoylated. To determine whether [^{3}H]palmitate was linked to the α4 and β2 nAChR subunits by hydroxylamine-sensitive thioester bonds, an IP sample from α4β2 lysate was run in parallel with an IP sample that was treated with hydroxylamine (Fig. 1*D*). The [^{3}H]palmitate was absent from the sample treated with hydroxylamine, indicating that labeling was due to palmitoylation of cysteine residues.

Cysteines in α4 nAChR Intracellular Loops Modulate Surface and Total α4β2 nAChR Protein Expression—To examine whether cysteine modifications altered α4β2 nAChR trafficking to the cell surface, the β2 subunit was coexpressed with either the WT α4, or with each of the α4 mutants (α4ΔC, α4ΔΔC, α4C273S) and processed for enzyme-linked immunoassay to detect protein expression at the cell surface. The absorbance data were normalized, and the WT α4 nAChR subunit was set to 100.0 ± 13.8%. Compared with the WT α4 nAChR subunit, α4ΔC (183 ± 20.9%, $p = 0.0006$), α4ΔΔC (206 ± 28.4%, $p = 0.001$), and α4C273S (120 ± 16.4%, $p = 0.006$) all significantly increased α4β2 nAChR surface expression (Fig. 2*A*, $n = 6$).

Parallel plates of tsA 201 cells were transiently transfected with β2 and α4, α4ΔC, α4ΔΔC, or α4C273S nAChR subunits. Samples were lysed, separated by SDS-PAGE, and analyzed by Western blotting with antibodies against FLAG (to detect α4), β2, or GAPDH to determine total steady-state protein expression levels. α4 nAChR protein levels were quantified by densitometry from five separate experiments and corrected for GAPDH expression. Data were normalized and WT α4 nAChR was set to 100 ± 30.3%. α4ΔC significantly increases total expression levels compared with α4, (202.1 ± 33.9%, $p = 0.02$), whereas α4ΔΔC increases protein expression but is not significant (200.6 ± 54.4%, $p = 0.11$). In contrast, α4C273S expression is decreased significantly (19.3 ± 4.1%, $p = 0.04$) compared with α4 ($n = 5$). A representative blot is shown (Fig. 2*B*).

Immunocytochemistry further verified the changes in α4β2 nAChR surface and total protein expression. tsA 201 cells were transfected transiently with the same plasmid combinations used in Fig. 2, *A* and *B*, and processed for immunocytochemistry. Single plane images were collected using identical settings. Cells were fixed and processed with or without permeabilization to qualitatively examine total or cell surface expression, respectively. The expression patterns observed by immunocytochemistry were comparable with those observed by cell surface and Western assays. All three of the mutants appeared to have increased surface immunostaining intensities when compared with the wt α4β2 nAChR (Fig. 2*C*, *top panels*). When cells were fixed and permeabilized with 0.2% Triton X-100 and imaged to detect total α4β2 nAChR expression, α4ΔC had increased staining intensity, α4ΔΔC had comparable intensity, and α4C273S had decreased total intensity compared with WT α4 (Fig. 2*C*, *bottom panels*). Taken together, these data show that mutating the cysteines in the M3-M4 loop increase both total and cell surface expression, whereas mutating the cysteine in the M1-M2 loop decreases total protein expression but increases surface expression compared with WT α4β2 nAChR levels.

2-Bromopalmitate Decreases Surface Expression of α4β2 nAChRs—The α4 nAChR subunit is palmitoylated in the M1-M2 loop, and this mutation decreases total protein expression while increasing surface protein expression. To address

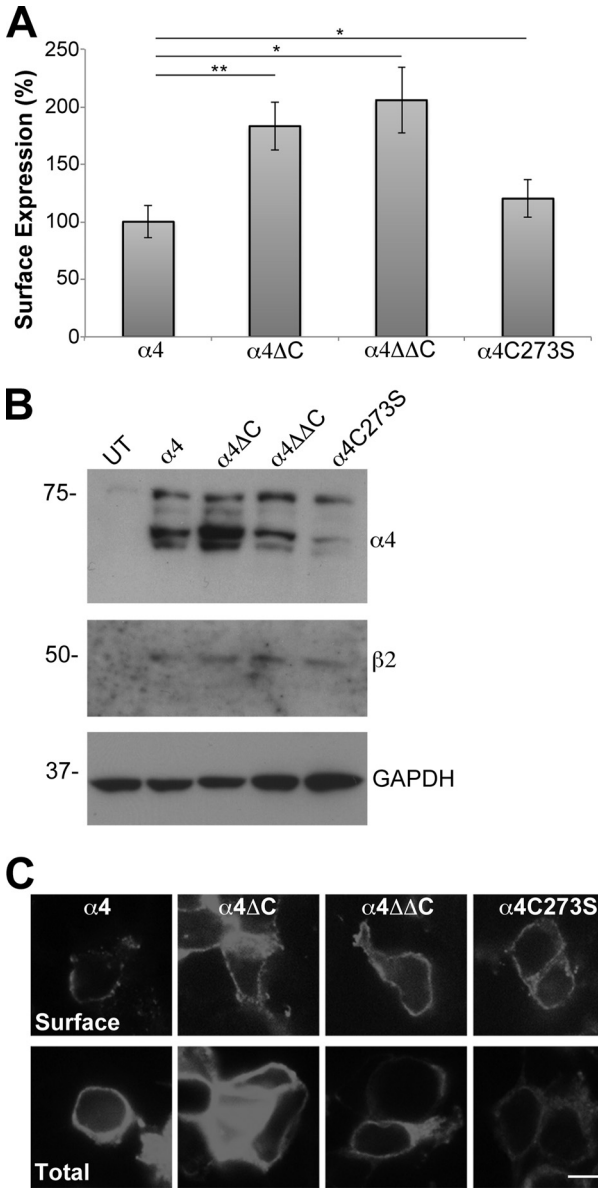

FIGURE 2. **Removal of cysteines from the α4 nAChR cytoplasmic loops increases the surface expression of the receptor.** *A*, tsA 201 cells were transfected with untagged β2 and N-terminally FLAG-tagged α4, α4ΔC, α4ΔΔC, or α4C273S nAChR subunits. Cell surface expression of α4β2 was measured using an enzyme-linked immunoassay using an mAb against the extracellular domain of the β2 nAChR subunit (mAb 295). The absorbance data were normalized, and the WT α4β2 nAChR was set to 100%, and data were expressed as means ± S.E. The α4ΔCβ2, α4ΔΔCβ2 and α4C273Sβ2 all had significantly higher surface expression than α4β2. *, $p < 0.05$; **, $p < 0.001$ ($n = 6$). *B*, transiently transfected tsA 201 cells were lysed in 750 μl of 2% Triton X-100 buffer. Soluble fractions (20 μl) were analyzed by SDS-PAGE and Western blotting. Blots were cut horizontally so that the same blot could be probed with either mouse monoclonal anti-FLAG antibody to detect the α4 nAChR, goat polyclonal anti-β2 antibody to detect the β2 nAChR or rabbit polyclonal anti-GAPDH antibody. Lysate from untransfected (*UT*) cells was run as a negative control. Molecular mass is in kDa along the *left side* of the blot. *C*, single-plane confocal images of transiently transfected tsA 201 cells were captured with a spinning disc confocal microscope. *Top panel*, to detect α4β2 nAChR expression on the cell surface, fixed, non-permeabilized cells were immunolabeled with mAb 295 followed by Alexa Fluor 594-conjugated goat anti-rat secondary antibody. *Bottom panel*, cells in a parallel set of wells were fixed, permeabilized, and immunolabeled with mAb 295 and Alexa Fluor 594-conjugated goat anti-rat secondary antibody to detect total α4β2 nAChR expression. All of the images were taken for the same exposure time with the same camera settings and processed identically. *Scale bar*, 10 μM.

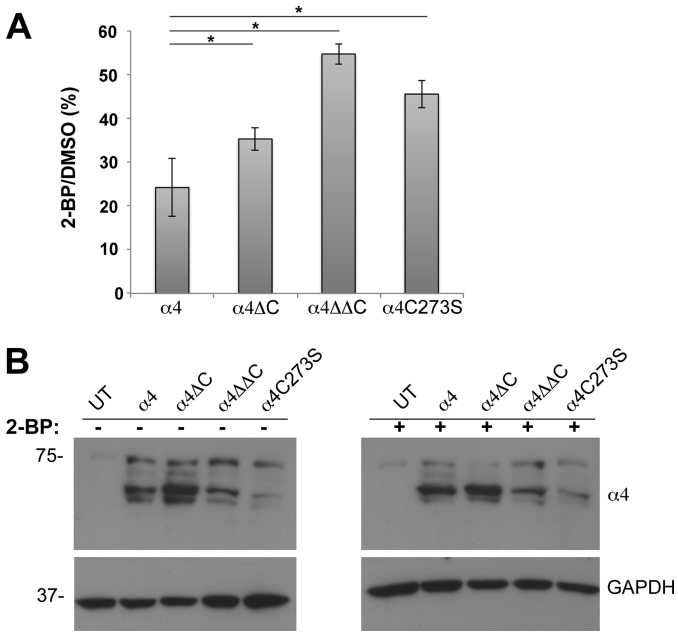

FIGURE 3. **2-Bromopalmitate significantly decreases the surface expression of α4β2 nAChRs.** *A*, tsA 201 cells were transfected with untagged β2 and N-terminally FLAG-tagged α4, α4ΔC, α4ΔΔC, or α4C273S nAChR subunits and incubated with 120 μM 2-BP or DMSO (vehicle control) overnight at 30 °C. Cell surface expression of α4β2 was measured using an enzyme-linked immunoassay using an mAb against the extracellular domain of the β2 nAChR subunit (mAb 295). The absorbance data were converted to expression ratios by dividing the 2-BP-treated cells by the DMSO-treated cells for each construct (expressed as percentages). 2-BP significantly decreased the surface expression of all of the constructs. The values are from three separate experiments and expressed as the means ± S.E. *B*, tsA 201 cells were transiently transfected with untagged β2 nAChR and with N-terminally FLAG-tagged α4, α4ΔC, α4ΔΔC, or α4C273S. The constructs were incubated with DMSO (vehicle control) (*left blots*, −) or with 120 μM 2-BP (*right blots*, +). The cells were lysed in 750 μl of 2% Triton X-100 buffer. Soluble fractions (20 μl) were analyzed by SDS-PAGE and Western blotting. Blots were cut horizontally, so that the same blot could be probed with either mouse monoclonal anti-FLAG antibody (to detect the α4 nAChR) or rabbit polyclonal anti-GAPDH antibody. Molecular mass is in kDa along the *left side* of the blot. *UT*, untransfected.

whether receptor depalmitoylation could stabilize the α4β2 nAChR at the cell surface, we blocked palmitoylation in cells transiently transfected with the β2 subunit and either the WT α4, α4ΔC, α4ΔΔC, or α4C273S. We examined cell surface expression using the immunoassay described in Fig. 2*A* in the absence or presence of 2-BP, a general palmitoylation inhibitor (Fig. 3*A*). The cell surface expression levels of vehicle (DMSO)-treated samples were set to 100%, and expression ratios for the 2-BP-treated samples were determined by dividing the absorbance values of the 2-BP-treated samples by the absorbance values of the DMSO-treated samples (WT α4β2, 23.9 ± 4.5%; α4ΔC, 35.2 ± 3.5%; α4ΔΔC, 54.6 ± 1.4%; α4C273S, 45.4 ± 2.4%, $n = 3$ (Fig. 3*A*)). The ratios were subtracted from 100% to determine the percent decrease in surface expression. All of the constructs decreased after treatment with 2-BP. Wild-type α4β2 decreased by 76.1 ± 4.5%, α4ΔC by 64.8 ± 3.5%, α4ΔΔC by 45.4 ± 1.4%, and α4C273S by 54.6 ± 2.4%.

If palmitoylation of α4 was the only variable in the experiment with 2-BP and if α4C273S affected expression only through an effect on palmitoylation, then the expected result with complete block of palmitoylation would be that 1) the expression ratio of wt α4β2 nAChR would equal the expression

ratio of α4ΔC because 2-BP would depalmitoylate both these constructs. In addition, 2) α4C273S and α4ΔΔC should not decrease (*i.e.* the expression ratios = 1) because they are already unable to be palmitoylated. Finally, 3) the α4C273S untreated mutant would equal the 2-BP-treated WT α4β2 nAChR because removing the palmitoyl group in the WT α4 nAChR subunit should make the two constructs equivalent. On the other hand, if palmitoylation of the α4 nAChR was the only variable in the experiment with 2-BP and if α4C273S intrinsically affected expression independent of palmitoylation, then 4) the untreated α4C273S and α4ΔΔC in the absence of 2-BP would be significantly different from the surface expression for α4ΔC and WT α4β2 nAChR in the presence of 2-BP because an effect other than palmitoylation is modulating the expression of the constructs.

These data do not meet expectation 1 (WT α4β2 and α4ΔC are significantly different, $p = 0.013$, $n = 3$), expectation 2 (both α4ΔΔC and α4C273S significantly decrease when treated with 2-BP), or expectation 3 (WT α4β2 decreases 76.1%, whereas α4C273S increases to 120%), but they do meet expectation 4 (α4C273S and α4ΔΔC increase in the absence of 2-BP, whereas α4ΔC and WT α4β2 nAChR decrease in the presence of 2-BP). Thus, these data suggest that palmitoylation of α4C273S is not the only variable affecting protein expression and that the effect of α4C273S may be independent of palmitoylation. Total protein expression was not affected by treatment with 2-BP, as determined by analysis of parallel samples by Western blotting (Fig. 3*B*).

Overall, these data show that 2-BP down-regulates α4β2 nAChR cell surface expression, consistent with previous ligand binding data (13). These findings suggest that $\alpha4Cys^{273}$ is important for cell surface expression but do not allow us to conclude that palmitoylation of $\alpha4Cys^{273}$ is responsible for the change in protein expression.

Cysteine Modifications Do Not Significantly Alter α4β2 nAChR EC_{50} or Ligand Binding Affinity—To determine whether the cysteine-to-serine amino acid replacement affects the EC_{50} of activation of the receptor, we compared the activation of WT to mutant receptors using a fluorescent assay that measures changes in intracellular calcium. The concentration response effects of epibatidine on WT or cysteine mutants show only relatively small differences in EC_{50} values (Fig. 4). The EC_{50} for the WT α4, α4ΔC, α4ΔΔC, and α4C273S are 25.2, 16.2, 23.7, and 20.2 nM, respectively (Table 1). These EC_{50} values are well within the published range for rat α4β2 nAChR functional data (18). There are no significant differences in EC_{50} values between the WT and mutant receptors, as determined by one-way ANOVA analysis.

We also compared the relative binding affinities of the receptors for nicotine in a competitive inhibition assay (Fig. 5). The K_i values were determined using a published K_d of 0.015 nM (17). No significant differences in the K_i values between α4 and α4-mutant containing receptors were seen (determined by one-way ANOVA), indicating that the intracellular cysteines do not affect ligand-binding affinity of surface receptors (Table 1). Thus, changes in the loop via cysteine mutations do not appear to significantly affect the EC_{50} or ligand-binding affinity of the α4β2 nAChR.

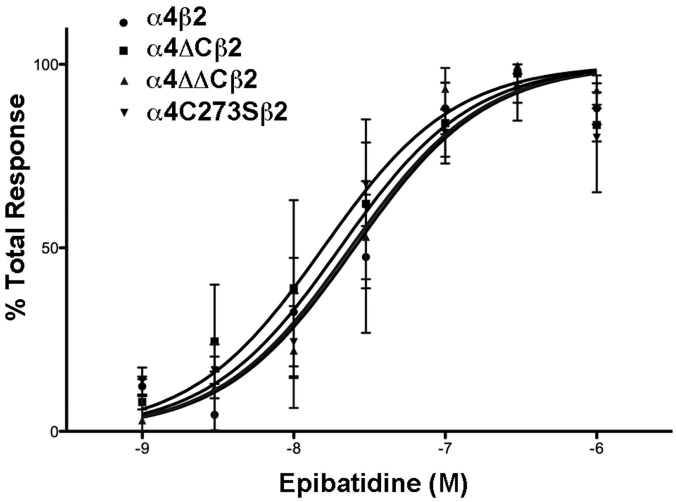

FIGURE 4. **There is no significant change in the EC_{50} for α4 nAChR cysteine mutants.** Cultured tsA 201 cells expressing the various α4 constructs plus β2 were loaded with calcium5 NW dye for 60 min, stimulated with either 1, 3, 10, 30, 100, 300, or 1000 nM epibatidine, and intracellular calcium was measured via fluorescence. Results are expressed as percentage of epibatidine peak fluorescence levels after subtracting basal fluorescence. Values represent means ± S.E., $n = 4$ for α4 and α4ΔC; $n = 3$ for α4ΔΔC and α4C273S. The data were fitted to a normalized dose-response curve using the equation $Y = 100/(1 + 10((\log EC_{50} - X)\cdot HS)$, where Y is the percentage of the maximal effect at a given concentration (X), and HS is the Hill slope (Hill slope = 1).

TABLE 1

EC_{50} values and ligand binding affinities for various α4β2 nAChR constructs

The experimental results from Figs. 4 and 5 are compiled in this table. EC_{50} values were derived from the equation: $Y = 100/(1 + 10((\log EC_{50} - X)\cdot HS)$, where Y is the percentage of the maximal effect at a given concentration (X), and HS is the Hill slope (Hill slope = 1). K_i values were derived from the one site − fit K_i equation in Prism 5 using a published K_d of 0.015 nM (17).

nAChR subtype	Functional potency		Ligand binding affinity	
	EC_{50}	n^a	K_i	n
	nM		nM	
α4β2	25.2 ± 6.1[c]	4	0.87 ± 0.16	6
α4ΔCβ2	16.2 ± 4.2	4	0.72 ± 0.11	5
α4ΔΔCβ2	23.7 ± 5.1	3	0.96 ± 0.16	3
α4C273Sβ2	20.2 ± 4.4	3	1.0 ± 0.16	3

[a] n = the number of independent experiments that were performed for each construct.

[b] Data are expressed as means ± S.E. There are no significant differences between the groups for EC_{50} or K_i, as determined by one-way ANOVA.

Cysteine Modifications Do Not Alter α4β2 nAChR Targeting in Neurons—We have shown previously that α4β2 nAChRs co-target with neurexin-1β to presynaptic terminals in rat hippocampal neuron cultures (15). Here, we tested whether the unpalmitoylated α4C273S subunit affected the targeting of the α4β2 nAChRs to synaptic terminals. Rat hippocampal neurons were transfected with neurexin-1β-VSV (nrx1β), β2 nAChR subunit, and WT α4 or α4C273S nAChR subunit cDNAs and then were cocultured with tsA 201 cells transfected with neuroligin-1-HA. As reported previously, the WT α4β2 nAChR does not accumulate at synaptic junctions (Fig. 6*A*). However, when it is coexpressed with neurexin-1β, the α4β2 nAChR co-targets with neurexin-1β to presynaptic terminals at junctions formed between neurexin-1β and neuroligin-1-HA (Fig. 6*B*). α4C273Sβ2 nAChRs also target to presynaptic terminals (Fig. 6*C*), suggesting that the C273S mutation is not important for α4β2 nAChR targeting to presynaptic terminals.

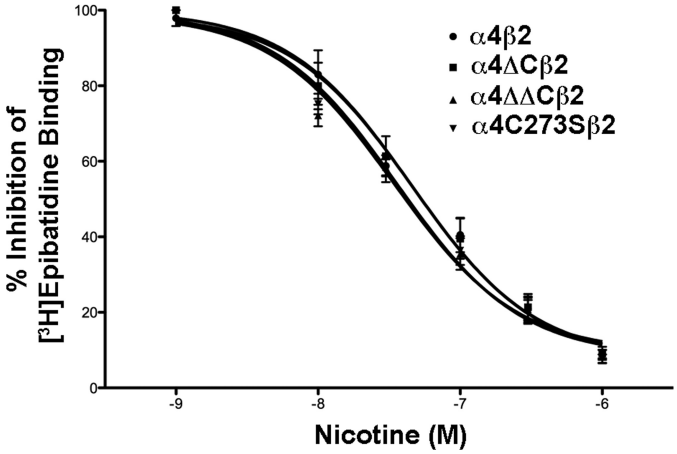

FIGURE 5. **Cysteine mutations in the α4 nAChR subunit do not affect α4β2 nAChR ligand binding affinity.** Cultured tsA 201 cells expressing the various α4 constructs plus β2 were fixed with paraformaldehyde, permeabilized, and incubated with 400 pM epibatidine in the presence or absence of 10, 30, 100, 300, or 1000 nM nicotine overnight at 4 °C. After several washes, the amount of bound epibatidine was quantified by scintillation counting. The data shown was normalized to the amount bound in the absence of nicotine and represent the mean ± S.E., $n = 6$ for α4; $n = 5$ for α4ΔC; $n = 3$ for α4ΔΔC and α4C273S. Curves were fitted to a one-site competitive binding using a K_d = 0.015 nM, using the equation $Y = 100/(1 + 10((\log IC_{50} - X)\cdot HS)$, where Y is the percentage of the maximal effect at a given concentration (X), and HS is the Hill Slope (Hill slope = 1).

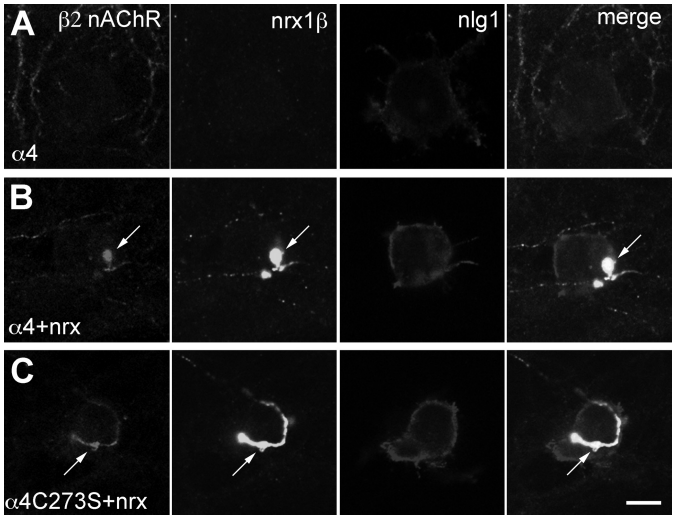

FIGURE 6. **Palmitoylation of the α4 nAChR subunit does not affect the targeting of the receptor to presynaptic terminals.** Single plane images of neurons that were transfected at 10 DIV, coplated with tsA 201 cells at 12 DIV and fixed, permeabilized, and immunostained at 14 DIV. *A*, neurons expressing α4β2 nAChRs were coplated with tsA 201 cells expressing neuroligin-1-HA (*nlg1*). *B*, neurons expressing α4β2 nAChRs and neurexin-1β VSV (nrx1β) were coplated with tsA 201 cells expressing neuroligin-1-HA. *C*, neurons expressing α4C273Sβ2 nAChRs and neurexin-1β were coplated with tsA 201 cells expressing neuroligin-1-HA. α4β2 nAChR and neurexin-1β-expressing cocultures exhibit enhanced targeting of α4β2 nAChRs to synapses (*arrows*). Antibody combinations were as follows: anti-β2 nAChR (mAb 295, *β2*), anti-VSV-G (*nrx1β*), and anti-HA (*nlg1*) antibodies. *Scale bar*, 10 μm.

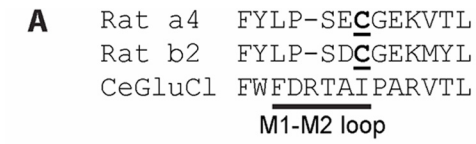

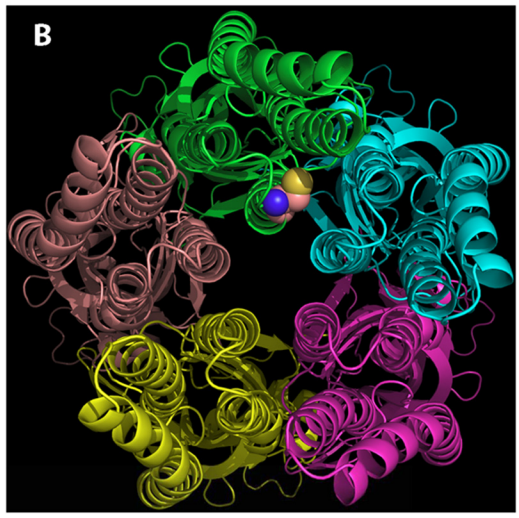

FIGURE 7. **The position of the palmitoylated cysteine likely allows ready access by the hydrophobic palmitoyl moiety to the hydrophilic cytoplasmic space and ion permeation path but does not allow ready access to the lipid bilayer.** *A*, the primary sequence comparison for α4, β2, and a Cys-loop receptor from *C. elegans* (19) shows the residues of and adjacent to the M1-M2 loop. The palmitoylated cysteine of α4 and homologous cysteine of β2 are *underlined*. The spatial position of $\alpha4Cys^{273}$ in *B* is based on this primary sequence homology and the x-ray crystal structure of the receptor from *C. elegans* (Protein Data Bank code 3RHW). *B*, as seen from the cytoplasmic side of the receptor from *C. elegans*, the likely position of $\alpha4Cys^{273}$ is adjacent to the transmembrane domains, the cytoplasmic space, and the ion permeation path at the center of the figure. Only the main chains of the subunits are displayed except for the homologous position of $\alpha4Cys^{273}$, which is displayed as a space-filling model of Cys at the distal end of the M1-M2 loop of the green chain. M1 is at the 9 o'clock position of the *green* chain, M2 is at 6 o'clock, and M3 is at 3 o'clock.

DISCUSSION

Palmitoylation is a post-translational modification that plays a significant role in the trafficking and function of many neuronal receptors. Previously, it has been reported that nAChRs are palmitoylated (13), but the specific palmitoylation sites have not been determined. Our study is the first to identify the site of palmitoylation on the α4 nAChR subunit as the sole intracellular cysteine in the M1-M2 cytoplasmic loop. Additionally, we found that this mutant decreases total protein levels but increases expression levels at the cell surface compared with the WT α4 nAChR. Surface expression also was increased in the mutant lacking all of the cysteines in the M3-M4 loop, but no palmitoylation sites were identified in this loop. Additionally, intracellular cysteines do not affect α4β2 nAChR ligand-binding affinity or localization to presynaptic terminals. Taken together, our findings suggest that cysteine residues, especially Cys^{273}, play a prominent role in receptor trafficking to the cell surface rather than in synaptic targeting or function.

Our study demonstrates that the α4 nAChR subunit undergoes palmitoylation and identifies the specific amino acid at position 273. This cysteine is located near the distal end of the short (about six residues) M1-M2 loop in certain nAChRs and is highly conserved across species and subunits, including α2, α3, α4, α6, β2, and β4 nAChR subunits and the 5HT3B subunit. Proposed physical mechanisms by which palmitoylation could exert its effects in membrane proteins include increasing the hydrophobic length of a transmembrane domain, associating with the lipid bilayer, and tilting of a transmembrane domain (4). The position of $\alpha4Cys^{273}$ at the distal end of the M1-M2 loop based on homology modeling with a Cys loop channel

from *Caenorhabditis elegans* (19) is closer to hydrophilic spaces of the cytoplasm and the ion permeation path than to the hydrophobic core of the membrane bilayer (Fig. 7). Access by the hydrophobic palmitoyl group on α4Cys^{273} to a preferred hydrophobic environment of the membrane bilayer or within the transmembrane domains of the nAChR subunits likely would distort the closely packed transmembrane domains. The position of α4Cys^{273} adjacent to the start of M2 suggests that more than one of the proposed physical mechanisms of palmitoylation effects might be relevant for $\alpha4\beta2$ nAChRs.

The C273S mutation leads to an increase in surface expression, but when the cells are treated with 2-BP, there is a decrease in $\alpha4\beta2$ nAChR cell surface expression. Why is there a discrepancy between the depalmitoylated mutant and using a palmitoylation inhibitor? 2-BP is a general palmitoylation inhibitor, so it inhibits the palmitoylation of many proteins in the cell beyond α4 nAChR subunits. A reasonable conclusion from the failure of expectations 1, 2, and 3 is that palmitoylation of α4Cys^{273} was not the only variable in the experiments with 2-BP, making the results impossible to interpret strictly in terms of palmitoylation of α4Cys^{273}. Additionally, 2-BP inhibits palmitoylation by an unknown mechanism of action and has been shown to have pleiotropic effects on other cellular functions including cellular metabolism (20). This generalized effect of 2-BP might impair the function of other proteins that traffic nAChRs to the cell surface. Alternatively, Cys^{273} may regulate cell surface stability independent of palmitoylation. Therefore, we are unable to say unequivocally that palmitoylation is necessary for the surface expression of $\alpha4\beta2$ nAChRs.

It is interesting to note that the cysteine that is palmitoylated in our study has been suggested to undergo reactive oxygen species-regulated use-dependent inactivation in the $\alpha3\beta4$ nAChR (14). The authors propose that use-dependent inactivation of the $\alpha3\beta4$ nAChR occurs after the receptors have been repeatedly exposed to agonist over time due to mild elevations in reactive oxygen species (14, 21, 22). Receptor use can also enhance the depalmitoylation of proteins (23–27). Although we observed similar EC_{50} and ligand-binding affinities between WT and mutant receptors, we have not examined whether use-dependent inactivation and depalmitoylation of the M1-M2 cysteine residue are linked. Future studies are necessary to address this question.

Our work provides two possible models for the cell surface trafficking of the $\alpha4\beta2$ nAChR. Compared with the wt α4 nAChR subunit, the $\alpha4\Delta C$ mutant has increased surface and total protein expression, suggesting that the increased surface expression is due to increased overall protein expression. The α4C273S mutant has decreased total protein expression compared with WT, but it still increases receptor expression at the cell membrane. $\alpha4\Delta\Delta C$ has increased surface expression but no change in total protein expression. These findings imply that the mutation of Cys^{273} to a serine either allows the receptor to pass through the secretory pathway more efficiently or impairs the internalization of the receptor, resulting in accumulation at the cell membrane. Further studies are necessary to determine which of these conclusions is correct, or if there is another explanation.

Changes in nAChRs expression levels are associated with many neurological diseases and disabilities, including nicotine addiction, autism, Alzheimer disease, Parkinson disease, schizophrenia, and diabetic neuropathies. Here, we have discovered a novel site of palmitoylation on the $\alpha4\beta2$ nAChR and determined that cysteine residues modulate nAChR trafficking to the cell surface. Our findings add to the literature on nAChR trafficking and may lead to new therapeutic strategies for altering nAChR cell surface expression in nAChR-associated diseases in the future.

Acknowledgments—We thank members of Dr. D. McKay's laboratory (The Ohio State University) for use of FLEXstation and Dr. J. Lindstrom (University of Pennsylvania) for supplying the β2 antibody.

REFERENCES

1. Millar, N. S. (2003) Assembly and subunit diversity of nicotinic acetylcholine receptors. *Biochem. Soc. Trans.* **31,** 869–874
2. Ren, X. Q., Cheng, S. B., Treuil, M. W., Mukherjee, J., Rao, J., Braunewell, K. H., Lindstrom, J. M., and Anand, R. (2005) Structural determinants of $\alpha4\beta2$ nicotinic acetylcholine receptor trafficking. *J. Neurosci.* **25,** 6676–6686
3. Xu, J., Zhu, Y., and Heinemann, S. F. (2006) Identification of sequence motifs that target neuronal nicotinic receptors to dendrites and axons. *J. Neurosci.* **26,** 9780–9793
4. Charollais, J., and Van Der Goot, F. G. (2009) Palmitoylation of membrane proteins (Review). *Mol. Membr. Biol.* **26,** 55–66
5. el-Husseini Ael-D., and Bredt, D. S. (2002) Protein palmitoylation: A regulator of neuronal development and function. *Nat. Rev. Neurosci.* **3,** 791–802
6. Greaves, J., Prescott, G. R., Gorleku, O. A., and Chamberlain, L. H. (2009) The fat controller: roles of palmitoylation in intracellular protein trafficking and targeting to membrane microdomains (Review). *Mol. Membr Biol.* **26,** 67–79
7. Shipston, M. J. (2011) Ion channel regulation by protein palmitoylation. *J. Biol. Chem.* **286,** 8709–8716
8. Hess, D. T., Patterson, S. I., Smith, D. S., and Skene, J. H. (1993) Neuronal growth cone collapse and inhibition of protein fatty acylation by nitric oxide. *Nature* **366,** 562–565
9. Hess, D. T., Slater, T. M., Wilson, M. C., and Skene, J. H. (1992) The 25-kDa synaptosomal-associated protein SNAP-25 is the major methionine-rich polypeptide in rapid axonal transport and a major substrate for palmitoylation in adult CNS. *J. Neurosci.* **12,** 4634–4641
10. Dunphy, J. T., and Linder, M. E. (1998) Signaling functions of protein palmitoylation. *Biochim. Biophys. Acta* **1436,** 245–261
11. Olson, E. N., Glaser, L., and Merlie, J. P. (1984) α and β subunits of the nicotinic acetylcholine receptor contain covalently bound lipid. *J. Biol. Chem.* **259,** 5364–5367
12. Drisdel, R. C., Manzana, E., and Green, W. N. (2004) The role of palmitoylation in functional expression of nicotinic α7 receptors. *J. Neurosci.* **24,** 10502–10510
13. Alexander, J. K., Govind, A. P., Drisdel, R. C., Blanton, M. P., Vallejo, Y., Lam, T. T., and Green, W. N. (2010) Palmitoylation of nicotinic acetylcholine receptors. *J. Mol. Neurosci.* **40,** 12–20
14. Campanucci, V., Krishnaswamy, A., and Cooper, E. (2010) Diabetes depresses synaptic transmission in sympathetic ganglia by inactivating nAChRs through a conserved intracellular cysteine residue. *Neuron* **66,** 827–834
15. Cheng, S. B., Amici, S. A., Ren, X. Q., McKay, S. B., Treuil, M. W., Lindstrom, J. M., Rao, J., and Anand, R. (2009) Presynaptic targeting of $\alpha4\beta2$ nicotinic acetylcholine receptors is regulated by neurexin-1β. *J. Biol. Chem.* **284,** 23251–23259
16. Jiang, M., and Chen, G. (2006) High Ca^{2+} phosphate transfection efficiency in low-density neuronal cultures. *Nat. Protoc.* **1,** 695–700
17. Marks, M. J., Smith, K. W., and Collins, A. C. (1998) Differential agonist

inhibition identifies multiple epibatidine binding sites in mouse brain. *J. Pharmacol. Exp. Ther.* **285,** 377–386
18. Buisson, B., Vallejo, Y. F., Green, W. N., and Bertrand, D. (2000) The unusual nature of epibatidine responses at the α4β2 nicotinic acetylcholine receptor. *Neuropharmacology* **39,** 2561–2569
19. Hibbs, R. E., and Gouaux, E. (2011) Principles of activation and permeation in an anion-selective Cys-loop receptor. *Nature* **474,** 54–60
20. Resh, M. D. (2006) Use of analogs and inhibitors to study the functional significance of protein palmitoylation. *Methods* **40,** 191–197
21. Campanucci, V. A., Krishnaswamy, A., and Cooper, E. (2008) Mitochondrial reactive oxygen species inactivate neuronal nicotinic acetylcholine receptors and induce long term depression of fast nicotinic synaptic transmission. *J. Neurosci.* **28,** 1733–1744
22. Krishnaswamy, A., and Cooper, E. (2012) Reactive oxygen species inactivate neuronal nicotinic acetylcholine receptors through a highly conserved cysteine near the intracellular mouth of the channel: Implications for diseases that involve oxidative stress. *J. Physiol.* **590,** 39–47
23. Wedegaertner, P. B., and Bourne, H. R. (1994) Activation and depalmitoylation of Gs α. *Cell* **77,** 1063–1070
24. El-Husseini Ael-D., Schnell, E., Dakoji, S., Sweeney, N., Zhou, Q., Prange, O., Gauthier-Campbell, C., Aguilera-Moreno, A., Nicoll, R. A., and Bredt, D. S. (2002) Synaptic strength regulated by palmitate cycling on PSD-95. *Cell* **108,** 849–863
25. Hayashi, T., Rumbaugh, G., and Huganir, R. L. (2005) Differential regulation of AMPA receptor subunit trafficking by palmitoylation of two distinct sites. *Neuron* **47,** 709–723
26. Hayashi, T., Thomas, G. M., and Huganir, R. L. (2009) Dual palmitoylation of NR2 subunits regulates NMDA receptor trafficking. *Neuron* **64,** 213–226
27. Noritake, J., Fukata, Y., Iwanaga, T., Hosomi, N., Tsutsumi, R., Matsuda, N., Tani, H., Iwanari, H., Mochizuki, Y., Kodama, T., Matsuura, Y., Bredt, D. S., Hamakubo, T., and Fukata, M. (2009) Mobile DHHC palmitoylating enzyme mediates activity-sensitive synaptic targeting of PSD-95. *J. Cell Biol.* **186,** 147–160